Cancer Letters xxx (2016) 1–10

Contents lists available at ScienceDirect

Cancer Letters

journal homepage: www.elsevier.com/locate/canlet

Original Article

Global profiling of viral and cellular non-coding RNAs in Epstein–Barr virus-induced lymphoblastoid cell lines and released exosome cargos

Alessia Gallo [a, *, 1], Serena Vella [a, 1], Monica Miele [b], Francesca Timoneri [b], Mariangela Di Bella [b], Silvia Bosi [b], Marco Sciveres [c], Pier Giulio Conaldi [a, b]

[a] Department of Laboratory Medicine and Advanced Biotechnologies, IRCCS-ISMETT (Istituto Mediterraneo per i Trapianti e Terapie ad alta specializzazione), Italy
[b] Fondazione Ri.MED, Italy
[c] Pediatric Hepatology and Liver Transplantation, IRCCS ISMETT, University of Pittsburgh Medical Center Italy, Palermo, Italy

ARTICLE INFO

Article history:
Received 5 October 2016
Received in revised form
1 December 2016
Accepted 2 December 2016

Keywords:
Epstein–Barr virus
Lymphoblastoid cell lines
miRNA
lncRNA
Exosomes

ABSTRACT

The human EBV-transformed lymphoblastoid cell line (LCL), obtained by infecting peripheral blood monocular cells with Epstein–Barr Virus, has been extensively used for human genetic, pharmacogenomic, and immunologic studies. Recently, the role of exosomes has also been indicated as crucial in the crosstalk between EBV and the host microenvironment. Because the role that the LCL and LCL exosomal cargo might play in maintaining persistent infection, and since little is known regarding the non-coding RNAs of LCL, the aim of our work was the comprehensive characterization of this class of RNA, cellular and viral miRNAs, and cellular lncRNAs, in LCL compared with PBMC derived from the same donors. In this study, we have demonstrated, for the first time, that all the viral miRNAs expressed by LCL are also packaged in the exosomes, and we found that two miRNAs, ebv-miR-BART3 and ebv-miR-BHRF1-1, are more abundant in the exosomes, suggesting a microvescicular viral microRNA transfer. In addition, lncRNA profiling revealed that LCLs were enriched in lncRNA H19 and H19 antisense, and released these through exosomes, suggesting a leading role in the regulation of the tumor microenvironment.

Introduction

The Epstein–Barr virus (EBV) is a ubiquitous γ-herpes virus that establishes life-long persistent infection in over 90% of the adult population worldwide, though usually without symptoms [68]. Once infection occurs, it is never cleared, residing in a subset of B lymphocytes for the lifetime of the host [6]. Latent EBV infection is associated with a wide range of human malignancies, including Burkitt's lymphoma, nasopharyngeal carcinoma, post-transplant lymphoproliferative disease, Hodgkin's lymphoma, and gastric carcinoma [35].

EBV is capable of driving B lymphocyte proliferation both *in vitro* to form immortalized cell lines, and *in vivo* when immune surveillance is inadequate [47].

Human EBV-transformed lymphoblastoid cell lines (LCL) are obtained by infecting peripheral blood mononuclear cells (PBMC) with EBV [57]. For the last few decades, this method has been successfully used, and LCL exhibit advantages, being easy to prepare and to maintain *in vitro*. In addition, they also exhibit chromosomal stability, with a minimal somatic mutation rate in continuous culture [55], and provide an unlimited source of biomolecules (DNA, RNA, or proteins). LCLs are widely used as a promising model system for human genetic, pharmacogenomic, and immunologic studies [9,37,39,60,65,67,72–74,76], and the applicability of LCLs for various clinical phenotypes is emerging [80,81].

Though LCLs are commonly used in various research fields, some concerns have been raised about their extensive use because of possible genetic changes during LCL generation, maintenance, and immortalization.

Abbreviations: LCL, lymphoblastoid cell lines; EBV, Epstein–Barr virus; PBMC, peripheral blood mononuclear cells; ncRNA, non-coding RNA; miRNA, micro-RNA; lncRNA, long non-coding RNA.

* Corresponding author. Department of Laboratory Medicine and Advanced Biotechnologies, ISMETT, Via Tricomi 5, 90127 Palermo, Italy. Fax: +39 091 21 92 422.
E-mail address: agallo@ismett.edu (A. Gallo).
[1] These authors made equal contributions as first author.

http://dx.doi.org/10.1016/j.canlet.2016.12.003
0304-3835/

For these reasons, to better characterize LCLs, many scientists have investigated biological and genetic features of these cell lines, focusing on identifying variations of EBV genes and microRNAs during the lytic cycle and latency, and their influence on the host [69].

Particular attention has been paid to the changes in cellular gene expression during the EBV-driven tumorigenesis [39], comparing gene expression profiles of LCLs at late ($p < 160$) passage compared with early passage (p4) [7,38], but little is known about the contribution of non-coding RNA (ncRNA) to LCL generation.

ncRNAs are functional RNA molecules that are transcribed but not translated into proteins, which regulate gene expression at the transcriptional and post-transcriptional levels. Among these, cellular microRNA (miRNA) and long non-coding RNA (lncRNA) have been studied in depth.

EBV was the first virus known to encode miRNAs [75], which regulate host cellular pathways [18,36,64]. Moreover, it has been demonstrated that exosomes secreted by LCLs contained both viral and human cellular miRNA [58,78], in addition to EBV proteins [51,53].

The aim of our work was a comprehensive characterization of LCLs to identify variations in the expression levels of EBV latent and lytic genes, cellular and viral miRNAs, and cellular lncRNAs in LCL compared with PBMC derived from the same donors.

Because it has been postulated that interactions between EBV and host microenvironment are relevant for the establishment of EBV latent infection in B cells [12,16], we characterized the ncRNA cargo contained within exosomes released *in vitro* by LCL, in order to shed light on possible and different mechanisms by which LCL could act in a paracrine way.

Materials and methods

Generation of viable EBV stock

EBV-transformed B95-8 marmoset cell line (85011419, Sigma–Aldrich Co., USA) was used for EBV stock preparation. The cells were seeded in RPMI-1640 (Lonza, Basel, Switzerland), 10% fetal bovine serum (FBS, Thermo Fisher Scientific, Waltham, MA, USA), 200 mM glutamine (Sigma–Aldrich Co.) After 7 days, confluent cultures of B95-8 appeared straw yellow in color and were split. The FBS concentration in the medium was then decreased to 5%, and to 2% subsequently. Finally the culture supernatant was collected by centrifugation and filtered through 0.22 μM filter (Millipore, Bedford, MA) to obtain EBV crude stock. The filtrate was aliquoted and stored − at 80 °C for long-term storage.

Samples and cell lines

Human blood samples, used in the present study for PBMC isolations and LCL derivations, came from healthy volunteers. This study was approved by our institute's Ethics Committee, and informed consent obtained from all the voluntary participants. The anonymous blood donors received oral and written information about the possibility that their blood would be used for research purposes. PBMC were isolated from whole blood samples by centrifugation at 1800×*g* for 28 min in BD Vacutainer CPT™ Cell Preparation Tube with Sodium Citrate (Becton Dickinson, Franklin Lakes, NJ). LCL were established by infecting fresh or thawed PBMC samples (typically $1–2 \times 10^7$) with EBV-concentrated cell culture supernatant from B95-8 [54] in RPMI-1640 (Lonza, Basel, Switzerland) supplemented with 10% fetal bovine serum (Hyclone FBS, Thermo Fisher Scientific, Waltham, MA, USA), 2 mM L-glutamine (Lonza) and 800 ng/ml cyclosporine A (Sandimmum, Novartis Pharma, Basel, Switzerland) to inhibit T lymphocyte proliferation. The B-cell blasts were split weekly for 1 month at a 1:2 ratio. LCL derivation was confirmed by cytofluorimetric analyses, evaluating the cell population positivity (≥80%) for CD19 (345791, BD Biosciences, Franklin Lakes, NJ) and CD20 (335811, BD Biosciences) antigens, and the cell population negativity for CD3 (552852, BD Biosciences) by Flow Cytometer (FACS Calibur, BD Biosciences).

Purification of exosomes from culture media

Exosomes were purified from supernatant through differential centrifugation, according to [21,22,46]. The conditioned supernatants were centrifuged at 1500×*g* for 10 min. The collected supernatant was centrifuged again at 17,000×*g* for 15 min, and the supernatant was spun again in an ultracentrifuge at 1,60,000×*g* for 1 h. All centrifugations were done at 4 °C.

The pelleted particles were washed and re-suspended in Qiazol (Qiagen, Germany) for RNA extraction, or in RIPA buffer (Thermo Fisher Scientific, Rockford, USA) for Western blot analysis or in PBS for Nanosight analysis.

NanoSight

Concentrations and size distribution were measured by Nanoparticle Tracking Analysis (NanoSight NS300, Malvern Instruments, Westborough, MA) at the ALFA-TESTlab (Cinisello Balsamo, Italy). Briefly, samples were diluted in phosphate buffered saline (PBS) 1:4000, manually injected into the instrument and videos acquired at ambient temperature. The measurement of exosome concentration performed in this study calculates particle size on a particle-by-particle basis in 5 videos to provide accuracy and statistics for each analysis.

Western blot

Purified exosomes or cells were treated with RIPA buffer and protease inhibitors (Protease Inhibitor Cocktail Set II, 539132, Calbiochem, EMD Chemicals, Merck KGaA, Darmstadt, Germany), and protein concentration was determined by Qubit® 3.0 Fluorometer (Life Technologies). Proteins were separated on 4–12% SDS–PAGE gel (Thermo Fisher Scientific, Rockford, USA) and transferred to PVDF membranes. Membranes were blotted overnight with antibodies against Alix (2171, Cell Signaling Technology, Denvers, CO, USA), or CD81 (sc-166028, Santa Cruz Biotechnology, Santa Cruz, CA), or GAPDH (sc-25778, Santa Cruz Biotechnology). The membranes were washed and incubated with anti-mouse (7076) or anti-rabbit (7074) HRP-conjugated secondary antibodies, purchased from Cell Signaling Technology. The signal was captured using a ChemiDoc XRS (BioRAD, CA).

RNA extraction. Reverse transcription (RT) and qPCR

Total RNA was isolated from LCL, PBMC, and exosomes using the miRNeasy Mini Kit (Qiagen), according to the manufacturer's instructions.

Analysis of EBV-encoded mRNAs

Expression of viral mRNA was quantified by TaqMan RT-PCR using ABI PRISM 7900 Fast instrument (Applied Biosystem, Thermo Fisher Scientific, Waltham, MA, USA) with the primer/probe combinations listed in Table 1. Total RNA was reverse-transcribed using High-Capacity cDNA Reverse Transcription Kit (Life Technologies, Thermo Fisher Scientific), according to manufacturer's instructions. cDNA was subsequently analyzed by qPCR. GAPDH was used as a reference gene for the relative quantification, assessed by $2^{-\Delta\Delta CT}$ calculation for each mRNA. All test samples were run in duplicate, and template-negative reactions served as controls.

EBV miRNA profiling

The viral profiling for EBV-miRNA expression was done using the Custom TaqMan® Array MicroRNA Cards (Life Technologies, Thermo Fisher Scientific), which includes 44 EBV miRNA in a 384-well format. Assay IDs are listed in Table 2. Total RNA was first reverse-transcribed with the Multiplex RT pool set (Life Technologies, Thermo Fisher Scientific) through a reverse transcription (RT) step using the TaqMan® MicroRNA Reverse Transcription Kit (Life Technologies, Thermo Fisher Scientific). The RT products were subsequently amplified with sequence-specific primers using the Applied Biosystems 7900 HT Real-Time PCR system according to the manufacturer's protocol. For each miRNA, the expression level was determined by the equation $2^{-\Delta\Delta CT}$. The heat map was generated using the ΔCT obtained from the amplification of all the 44 viral miRNAs with quantitative RT-PCR.

TaqMan low-density arrays (TLDA) for miRNAs profiling

MicroRNA profiling of samples was done with TaqMan Array Human MicroRNA panels A and B (Life Technologies, Thermo Fisher Scientific) to analyze 754 human miRNAs. Reverse transcription and pre-amplification were done following the manufacturer's instructions (Life Technologies, Thermo Fisher Scientific). QRT-PCR was performed with the Applied Biosystems 7900 HT Real-Time PCR system. For each miRNA, the expression level was determined by the equation $2^{-\Delta\Delta CT}$. Gene Expression Suite software (v1.0.4) and Data Assist software (v 3.01) (Life Technologies, Thermo Fisher Scientific) were further used to process the array data.

LncRNA expression profiling

The expression of 90 lncRNAs was identified using the LncProfiler™ qPCR Array Kit (SABiosciences, System Biosciences, Mountain View, CA). RNA from cells ($n = 4$ per each group) were reverse transcribed using RT^2 First Strand Kit (SABiosciences, Qiagen, Valencia, CA), according to the manufacturer's instructions. QRT-PCR was performed (SABiosciences RT^2 qPCR Master Mix, Qiagen), and the cycle number at which the reaction crossed a threshold (Ct) was determined for each lncRNA. GAPDH was used as a reference gene for the relative quantification, assessed by $2^{-\Delta\Delta CT}$ calculation for each lncRNA.

Data analysis and statistical analysis

Data processing and analysis were done with tools from RQ-manager (v1.2, Life Technologies, Thermo Fisher Scientific), Expression Suite software (v1.0.4, Life Technologies, Thermo Fisher Scientific), Microsoft Excel and Prism GraphPad V5.0d software (GraphPad Software, CA). Heat maps were constructed using DataAssist software (v3.01, Life Technologies, Thermo Fisher Scientific).

Statistical significance of observed differences among different experimental groups was calculated using a two-tailed unpaired Student's *t*-test. P-values of <0.05

Please cite this article in press as: A. Gallo, et al., Global profiling of viral and cellular non-coding RNAs in Epstein–Barr virus-induced lymphoblastoid cell lines and released exosome cargos, Cancer Letters (2016), http://dx.doi.org/10.1016/j.canlet.2016.12.003

Table 1
Primers and Probes for Lytic and Latent EBV Genes.

Target	Forward	Reverse	Probe
BHRF1	GCAGGACATTGTGTTGTAACCAG	TAATGTAGACCAGCCGCCCT	CTACTCCTTACTATGTTGTGGACCTGTCAGTTCGTG
BZLF1	CCCAAGCCTGGATGTTGACT	GAAGCAGGCGTGGTTTCAAT	CATTATCCCCCGGACACCAGATGTTTTACA
BLLF1	AGAATCTGGGCTGGGACGTT	ACATGGAGCCCGGACAAGT	AGCCCACCACAGATTACGGCGGT
EBNA1	AGGATGCGATTAAGGACCTTGTT	CCATCGTCAAAGCTGCACAC	TGACAAAGCCCGCTCCTACCTGCAATA
EBNA2	CGGCAACCCCTAACGTTTC	GGGAAGAGAATGGGAGCCTC	CCAATACATGAACCGGAGTCCCATAATAGCC
EBNA3A	GTGGCACTTGAGCGACCAG	TAATGCCAGAAGTTTCCCCG	TTACCCCAAGCCAGTTCGTCCGG
EBNA3B	GGGCACATTCCATATCAGCC	CTCTCGGTGGTGTCTGCATG	ACCAACGGGTCCTGCTACCATGCTGT
EBNA3C	CAAGGTGCATTTACCCCACTG	GGGCAGGTCCGTGAGAACT	CATTAATGCCACCACGCCAAAAAGGC
LMP1	TCCTCCTGTTTCTGGCGATTT	GGGAGTCATCGTGGTGGTGT	AATCTGGATGTATTACCATGGACAACGACACA
LMP2A	CCGTCACTCGGACTATCAAC	TGAGATGAGTCATCCCGTGGA	TCATTCCCGTCGTGTTGCAATCCCAAGTACAG
EBER	AGGACCTACGCTGCCCTAGAG	AACCACAGACACCGTCCTCAC	AGCCACACACGTCTCCTCCCTAGCAAA
BARTs	GCCTGGCGGACTTCATTCT	TCTCCTGTAACCACCTGGCG	ACAGTCCCGAGACCGGCTCCG

were considered to be statistically significant. In the Figures, * and ** indicate statistical significance at $p < 0.05$ and 0.01, respectively.

Results

EBV miRNA and gene expression profile in LCL and PBMC

The autologous LCL were obtained after infection of the B cells by EBV released from the marmoset cell line B95-8, as described by Miller et al. [53].

Cytofluorimetric analyses confirmed that cells from LCL showed expression of typical B-cell surface markers (CD19 and CD20), while the marker for T-cell (CD3) was absent (data not shown), thus ascertaining the purity of growing cultures.

In order to confirm that the obtained cell lines contained the genetic arrangement of EBV B95-8 strain, we checked for the presence of viral miRNAs. Fig. 1A shows the heat map relative to the viral miRNA expression levels, normalized to U6 snRNA, in PBMC isolated from healthy individuals (n = 4) and autologous LCL (n = 4). As expected, PBMC of healthy volunteers did not express any EBV miRNA, while in the autologous LCL, of 44 miRNA, only a part of them were amplified (EBV- miR-BHRF1-1, miR-BHRF1-2 and miR-BHRF1-3 of the BHRF cluster, ebv-BART1-3p, BART1-5p, BART2-5p, BART3, BART3*, BART4 and BART15 of the BART cluster) (Table S1). These results are consistent with the deletion of 12 Kb in the BamHI-A region carried from the B95.8 strain [70].

We also evaluated the expression level of the viral genes, of both the lysis and latency phases, in PBMC (n = 4) and autologous LCL (n = 4). As shown in Fig. 1B, both lytic and latency genes were highly expressed in the autologous LCL, while PBMC showed no expression of viral transcripts (Table S2).

Table 2
Q7 Assay IDs for EBV miRNAs.

Assay name	Assay ID	Assay name	Assay ID
ebv-miR-BART1-3p	464048_mat	ebv-miR-bart13*	006990
ebv-miR-bart1-5p	197199_mat	ebv-miR-bart14	006386
ebv-miR-bart2-3p	006174	ebv-miR-bart14*	005811
ebv-miR-bart2-5p	197238_mat	ebv-miR-bart16	006319
ebv-miR-BART3	004578_mat	ebv-miR-bart17-3p	008119
ebv-miR-BART3*	004432_mat	ebv-miR-bart17-5p	008216
ebv-miR-bart4	005623	ebv-miR-bart18-3p	008473
ebv-miR-bart5	197237_mat	ebv-miR-bart18-5p	008081
ebv-miR-bart5*	006342	ebv-miR-bart19-3p	197235_mat
ebv-miR-bart6-3p	008317	ebv-miR-bart19-5p	006693
ebv-miR-bart6-5p	005531	ebv-miR-bart20-3p	007266
ebv-miR-bart7*	005711	ebv-miR-bart20-5p	006851
ebv-miR-bart8	008211	ebv-miR-bart21-3p	006186
ebv-miR-bart8*	197196_mat	ebv-miR-bart21-5p	006882
ebv-miR-bart9	007435	ebv-miR-bart22	006609
ebv-miR-bart9*	006884	ebv-miR-bhrf1-1	007757
ebv-miR-BART10	004421_mat	ebv-miR-bhrf1-2	197239_mat
ebv-miR-bart11-3p	197210_mat	ebv-miR-bhrf1-2*	006088
ebv-miR-bart11-5p	005755	ebv-miR-bhrf1-3	197221_mat
ebv-miR-bart12	005725	RNU48	001006
ebv-miR-bart13	005446	U6 snRNA	001973

Host PBMC cell miRNome significantly changes after EBV infection

To study the effect of EBV infection on the miRNA expression profile (miRNome) of PBMC cells, we analyzed miRNA expression by qRT-PCR arrays in human PBMC isolated from healthy individuals (n = 4) and autologous LCL (n = 4). The transformation of the B cells into LCL driven by the EBV B95.8 strain created a very specific pattern of miRNAs (Supplementary Tables S3 and S4), as shown in Fig. 1C and D. The samples clustered strongly and, among the analyzed miRNAs, some presented a presence/absence pattern.

Among 754 human miRNAs on the arrays (panels A and B), 24 were significantly up-regulated (Table 3), while 50 were down-regulated (Table 4) in LCL compared with PBMC.

Analysis of differentially expressed lncRNAs in LCL and PBMC

Since many studies have shown that lncRNAs play key roles in several diseases, including cancer [23,41], we investigated the possible role of lncRNAs in the process of transformation of PBMC into LCL driven by B95.8 EBV. We used the LncProfiler™ qPCR to check the expression of 90 lncRNAs in human PBMC isolated from healthy individuals and autologous LCL. Of the 90 lncRNAs tested, we selected only those (14) with a clearly distinguishable single-peak melting (Tm). Among these, only 4 showed a significant differential pattern between the two groups (Fig. 1E, Supplementary Table S5). Indeed, 7SL, H19, H19 antisense ($p < 0.01$) and p53 mRNA ($p < 0.05$) showed a higher expression in the autologous LCL when compared with the PBMC.

Characterization of the exosome cargo released from autologous LCL

Communication between cells and the microenvironment through exosome-mediated transfer of proteins, microRNA, or mRNA to the recipient cells has been shown by multiple means [51,58].

To determine the miRNA repertoires of exosomes secreted by LCL, we first isolated exosomes from cell supernatants through a series of ultracentrifugation steps.

The medium used to culture the LCL contains 10% fetal bovine serum, and, even if in a very low percentage, the serum exosomal cargo might affect the output of the experiment. Indeed, it has been demonstrated that FBS also contains several regulatory RNA species, including mRNA, miRNA, rRNA, and snoRNA, which might interfere with the downstream RNA analysis and lead to false results and interpretation [79].

Please cite this article in press as: A. Gallo, et al., Global profiling of viral and cellular non-coding RNAs in Epstein–Barr virus-induced lymphoblastoid cell lines and released exosome cargos, Cancer Letters (2016), http://dx.doi.org/10.1016/j.canlet.2016.12.003

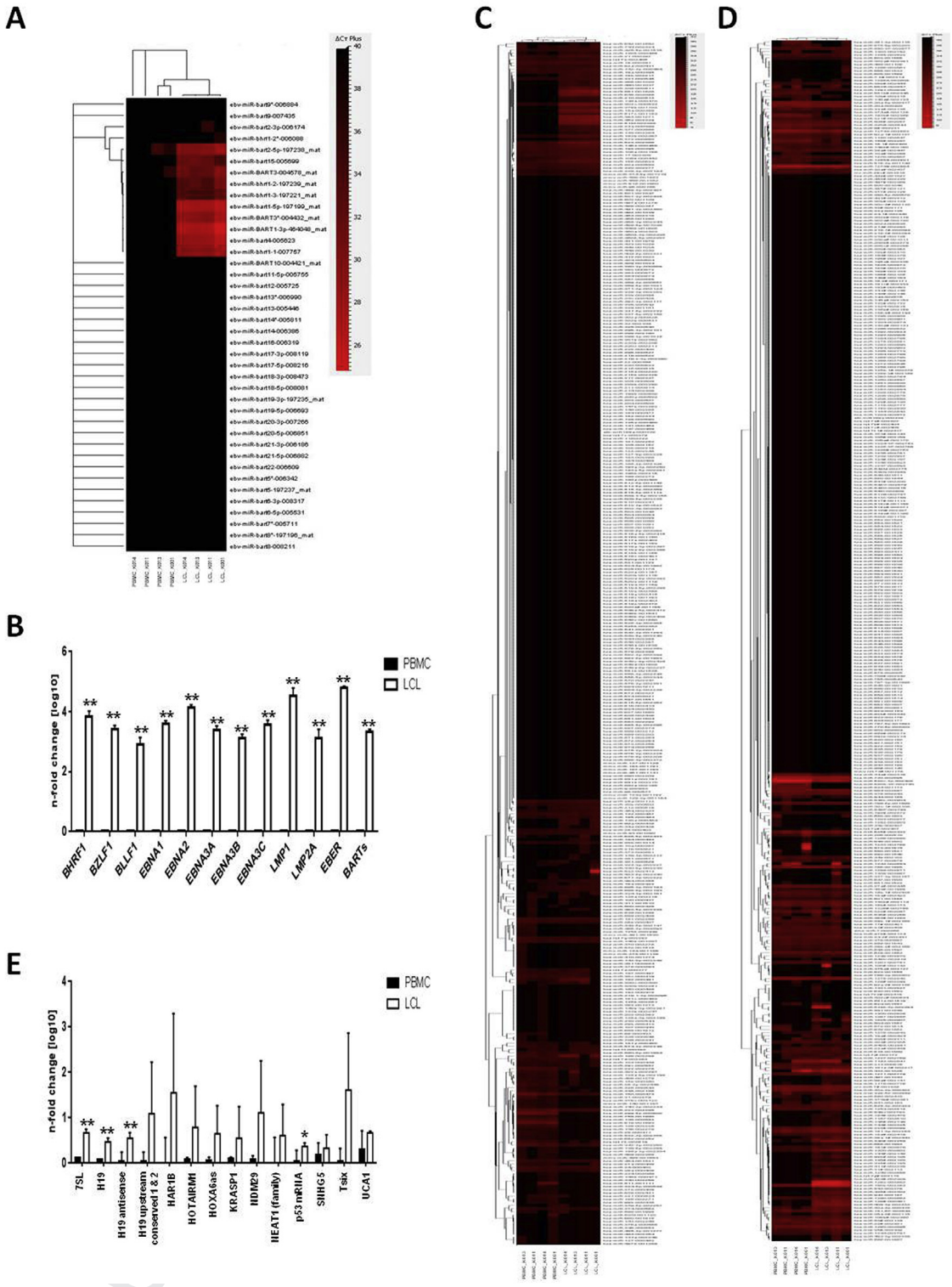

Fig. 1. A. Expression profile of EBV-specific microRNAs in LCL (n = 4) and PBMC (n = 4) samples. Expression data of 44 viral miRNAs were obtained with Custom TaqMan® Array MicroRNA Cards (Life Technologies. Thermo Fisher Scientific), analyzed using RQ-manager (v1.2) and DataAssist (v3.01), and shown in the heat map. The distance measured is Pearson's Distance, and the clustering method is average linkage. Each column corresponds to the sample expression profile, and each row corresponds to a miRNA. The miRNA clustering tree is shown on the left. Branch lengths represent the degree of similarity between individual miRNAs. Red and black colors indicate relatively high and low expression, respectively. **B**. LCL express EBV latent and lytic transcripts. The figure shows quantitative RT-PCR results of RNA extracted from LCL (n = 4) and PBMC (n = 4). Results are displayed as mean levels and SD relative to the average expression of PBMC, and are normalized to GAPDH. Two stars (**) indicate $p < 0.001$ on two-tailed Student's test. **C and D**. Unsupervised hierarchical clustering and analysis of miRNA expression profiles differentiate LCL (n = 4) from PBMC (n = 4). Cellular microRNA (miRNA) expression patterns were examined using microfluidic cards containing TaqMan probes and primer pairs (TaqMan® Low Density Array. TLDA) for 754 human mature miRNAs (pool A and pool B, Figure **C** and **D**, respectively). The samples were grouped by unsupervised hierarchical clustering on the basis of similarity in expression patterns. Branch lengths represent the degree of similarity between individual samples (Top) or miRNA (Left). Each column corresponds to the expression profile of samples, and each row corresponds to a miRNA. The colour reflects the level of expression of the corresponding miRNA in the corresponding sample relative to its mean level of expression in the entire set of PBMC samples. The distance measured is Pearson's Distance, and the clustering method is

Please cite this article in press as: A. Gallo, et al., Global profiling of viral and cellular non-coding RNAs in Epstein–Barr virus-induced lymphoblastoid cell lines and released exosome cargos, Cancer Letters (2016), http://dx.doi.org/10.1016/j.canlet.2016.12.003

Table 3
Cellular miRNAs up-regulated in LCL versus PBMC.

	P value	Mean 1	Mean 2	Difference	SE of difference	t ratio
hsa-miR-452	1.18E−07	1	259105	−259104	9027.04	28.7031
hsa-miR-377	1.45E−07	1	251.605	−250.605	9.03022	27.7518
hsa-miR-524	3.57E−06	1.02913	22489.1	−22488.1	1391.69	16.1589
hsa-miR-517c	4.12E−05	1	1876.19	−1875.19	176.643	10.6157
hsa-miR-302c	9.86E−05	1.01608	373.953	−372.937	40.9606	9.10476
hsa-miR-23a	0.000204	1	235.136	−234.136	29.2736	7.99821
hsa-miR-376b	0.000702	1	1830.92	−1829.92	287.196	6.37168
hsa-miR-9#	0.001126	1.39074	13.7732	−12.3824	2.12577	5.82491
hsa-miR-208	0.001588	1	2835.75	−2834.75	520.153	5.44985
hsa-miR-561	0.00209	1	327027	−327026	63350.9	5.16214
hsa-miR-636	0.003224	1	48656	−48655	10286.1	4.73019
hsa-miR-363	0.003321	1	269872	−269871	57399.8	4.70161
hsa-miR-210	0.00341	1	204.645	−203.645	43.5509	4.67601
hsa-miR-34a#	0.003907	1.25078	66.6972	−65.4464	14.3952	4.54642
hsa-miR-516-3p	0.005246	10.6103	76.4314	−65.8211	15.404	4.27299
hsa-miR-155#	0.008346	15.5516	74.2966	−58.745	15.2121	3.86172
hsa-miR-551b#	0.009003	1.02913	961.839	−960.809	253.067	3.79666
hsa-miR-193b#	0.017621	4.45319	109.786	−105.333	32.4802	3.24299
hsa-miR-372	0.024259	1	52.5515	−51.5515	17.23	2.99196
hsa-miR-18b	0.025324	5.94412	61.0953	−55.1511	18.64	2.95876
hsa-miR-1255B	0.030074	1.21154	3.08967	−1.87813	0.664342	2.82706
hsa-miR-15a	0.038271	1	42042.5	−42041.5	15893.2	2.64525
hsa-miR-1274A	0.04555	1.50704	5.63672	−4.12968	1.64155	2.51572
hsa-miR-10a#	0.048928	1.02913	186.949	−185.92	75.4888	2.46289

To address this, we ran the same experiment on RNA samples isolated using the same procedure from the corresponding fresh non-conditioned medium, which it has been considered as a negative control, as suggested by Wei Z et al. [79].

Exosome identity and purity was assessed by NanoSight and Western blot analysis (Fig. 2A and B).

Though the majority of LCL is latently infected with EBV, few cells (about 5–7%) may release active viruses [52], which could contaminate exosome preparations, because virus particles have similar size and density to exosomes [13,27,62]. To monitor viral contamination and purity of exosome preparations, pellets were analyzed by Nanosight.

Fig. 2A shows the presence of particles in the expected exosomal size range (average 92.6 ± 1.6 nm), clearly different to EBV size (150–200 nm, [77]), confirming the absence of viral particles in our exosome preparations.

In addition, to better characterize the exosomial fraction, we performed Western-blot analysis for the two universal exosomal markers Alix and CD81 [46], which, as expected, were found only in exosome samples [10,33], while GAPDH, a ubiquitously expressed protein, was found in both cellular and exosomal fractions.

After ascertaining exosome preparation purity, RNA was extracted and RNA integrity and gDNA contamination were verified (data not shown). For each sample, the expression of 754 cellular microRNAs was analyzed by TaqMan Array Human MicroRNA panels A and B.

We found 138 miRNAs in exosomes isolated from the fresh medium (mainly expressed at very low expression levels), and to subtract this FBS RNA contribution to each RNA sample, we normalized all qRT-PCR data to those of exosomes of fresh medium.

Interestingly, we assessed the presence of 304 miRNAs of the 754 cellular microRNAs (Supplementary Table S6). Non-hierarchical clustering of all expressed microRNAs again defined one clear cluster when compared with the exosomes isolated from the medium in which the cells were grown (Fig. 2C and D).

Looking at the viral pattern, notable is the presence of the miRNAs of the BHRF cluster, ebv-miR-BHRF1-1, miR-BHRF1-2 and miR-BHRF1-3, known to be important in malignant B-cell transformation. We found ebv-miR-BART1-3p, miR-BART1-5p, miR-BART2-5p, miR-BART3, miR-BART3*, miR-BART4 and miR-BART15 of the BART cluster also present, while, in the non-conditioned medium, none of the EBV viral miRNA were found (Fig. 2E). Furthermore, we wanted to explore the possibility of a specific viral miRNA packaging process in the exosomes. To address this question, we compared the viral miRNA expression of the exosomes with the LCL. We found that 2 miRNAs, ebv-miR-BART3 and ebv-miR-BHRF1-1, are highly differentially expressed, with a 3607.8-fold change ($p = 0.03$) and 255.5-fold change ($p = 0.03$), respectively (Fig. 2F).

We decided to verify the presence of the lncRNAs found in the LCL by which we isolated the exosomal fraction. We found 9 lncRNAs in the LCL exosome cargo: 7SL, H19, H19 upstream conserved 1&2, H19 antisense, HAR1B, HOXA6as, NDM29, SNHG5, and Tsix (Supplementary Table S7).

These lncRNAs were present at lower levels in exosomes with respect to what was observed for LCL, with the exception of H19 and H19 antisense (Fig. 2G).

Discussion

The human EBV-transformed LCL, obtained by infecting PBMC with EBV, has been extensively used for human genetic, pharmacogenomic, and immunologic studies, and, lately, for therapies, with LCL used as antigen-presenting cells that can efficiently stimulate EBV-specific T-cells. Nevertheless, little is known regarding the contribution of ncRNA to LCL generation. In this study, we aimed to characterize the comprehensive ncRNA content of LCL. We used 4 LCL obtained after infection of the B cells with EBV propagated in the marmoset cell B95-8, which display a latency III gene expression pattern. The data were compared with

average linkage. The increasing intensities of red mean that a specific miRNA has a higher expression in the given sample, and the increasing intensities of black mean that this miRNA has a lower expression. **E**. LCL differentially express cellular long non-coding RNAs. The graph shows quantitative RT-PCR results of RNA extracted from LCL (n = 4) and PBMC (n = 4). Results are shown as mean levels and SD relative to the average expression of PBMC controls, and are normalized to GAPDH. One star (*) indicates a $p < 0.05$, while two stars (**) indicate a $p < 0.001$ on two-tailed Student's test. (For interpretation of the references to colour in this figure legend, the reader is referred to the web version of this article.) Q10

Please cite this article in press as: A. Gallo, et al., Global profiling of viral and cellular non-coding RNAs in Epstein–Barr virus-induced lymphoblastoid cell lines and released exosome cargos, Cancer Letters (2016), http://dx.doi.org/10.1016/j.canlet.2016.12.003

Table 4
Cellular miRNAs down-regulated in LCL versus PBMC.

	P value	Mean 1	Mean 2	Difference	SE of difference	t ratio
hsa-miR-136	0.000775	1.03563	0.000139	1.0355	0.165559	6.25454
hsa-miR-299-5p	0.000813	1.0401	0.001998	1.03811	0.167481	6.19833
hsa-miR-30c	0.000843	1.01437	0.248213	0.766162	0.124468	6.15549
mmu-miR-140	0.000853	1.03535	0.004325	1.03102	0.167867	6.14189
hsa-miR-140-3p	0.000927	1.04457	0.009848	1.03473	0.17115	6.04574
hsa-miR-574-3p	0.001586	1.00138	0.352542	0.648842	0.119032	5.45101
hsa-miR-758	0.001833	1.0571	0.002321	1.05478	0.19908	5.29827
hsa-miR-518f	0.001912	1	99698.9	−99697.9	18974	5.25446
hsa-miR-223	0.002018	1.02887	0.114521	0.914352	0.175894	5.19833
hsa-miR-652	0.003138	1.06272	0.005337	1.05738	0.222308	4.75639
hsa-miR-28	0.00374	1.10619	0.004858	1.10133	0.240059	4.58775
hsa-miR-181a	0.003984	1.01991	0.225396	0.794518	0.17547	4.52793
hsa-miR-26b	0.004812	1.04731	0.206111	0.841203	0.193294	4.35193
hsa-miR-191	0.004991	1.02162	0.263126	0.758497	0.175643	4.31839
hsa-miR-376c	0.006956	1.1275	0.006802	1.1207	0.278755	4.02038
hsa-miR-146b	0.007034	1.00294	0.313499	0.689438	0.171907	4.01053
hsa-miR-28-3p	0.00729	1.07033	0.094065	0.976267	0.245347	3.97913
hsa-let-7g#	0.007581	1.1029	0.004526	1.09837	0.278423	3.94498
hsa-miR-618	0.008508	1.09266	9.11E-06	1.09265	0.284163	3.84516
hsa-miR-520f	0.009036	1.10121	6.15E-05	1.10115	0.290273	3.79349
hsa-miR-486	0.009129	1.08575	0.124502	0.961246	0.253976	3.78479
hsa-miR-942	0.01088	1.11442	0.000171	1.11425	0.306405	3.63653
hsa-miR-191#	0.011571	1.0834	0.098219	0.985182	0.274796	3.58514
hsa-miR-31#	0.011811	1.14222	0.000133	1.14208	0.32008	3.56812
hsa-miR-543	0.012	1.13187	0.00017	1.1317	0.318344	3.55496
hsa-miR-15b	0.012397	1.15671	0.003333	1.15338	0.326914	3.52807
hsa-miR-342-3p	0.012765	1.10707	0.107975	0.999099	0.285135	3.50395
hsa-let-7g-	0.013104	1.06182	0.270893	0.790923	0.227118	3.48243
hsa-miR-29c	0.016479	1.05164	0.275901	0.775734	0.23532	3.29651
hsa-miR-425#	0.016593	1.11611	0.000118	1.11599	0.339103	3.29102
hsa-miR-150	0.020232	1.19623	0.013331	1.1829	0.377487	3.13361
hsa-miR-497	0.020534	1.22985	0.003866	1.22599	0.392702	3.12193
hsa-miR-432	0.020674	1.23198	0.00013	1.23185	0.395254	3.11661
hsa-miR-1249	0.025417	1.25902	0.000511	1.25851	0.425757	2.95593
hsa-miR-106b#	0.029032	1.23684	0.065682	1.17116	0.410367	2.85392
hsa-miR-1197	0.030244	2.87797	0.034597	2.84337	1.0073	2.82278
hsa-miR-145	0.033287	1.24243	0.006303	1.23613	0.449486	2.7501
hsa-miR-1825	0.034949	16.1547	0.000166	16.1545	5.95367	2.71337
hsa-miR-328	0.035777	1.25409	0.083683	1.17041	0.434167	2.69576
hsa-miR-126	0.036323	1.28891	0.000818	1.28809	0.479845	2.68439
hsa-miR-345	0.037257	1.13902	0.134421	1.0046	0.376912	2.66534
hsa-miR-30a-3p	0.037636	1.23526	0.094307	1.14095	0.42929	2.65777
hsa-miR-532-3p	0.038021	1.19836	0.007921	1.19044	0.449194	2.65016
hsa-miR-425-5p	0.039937	1.24345	0.282401	0.96105	0.367737	2.61342
hsa-miR-132	0.040168	1.2078	0.136375	1.07143	0.410648	2.60911
hsa-miR-31	0.041343	1.3715	0.000815	1.37068	0.529703	2.58764
hsa-let-7d	0.043562	1.30736	0.161636	1.14572	0.449517	2.54879
hsa-miR-125a-5p	0.04575	1.34371	0.004631	1.33907	0.532969	2.51248
hsa-miR-424#	0.047954	1.27368	0.000352	1.27333	0.513915	2.47771
hsa-miR-1227	0.049412	1.30793	0.178694	1.12923	0.459856	2.45562

those of PBMC derived from the same donors, as previously reported by several studies [26,31,43,49,56,66,85].

We focused our attention on different classes of ncRNA, both cellular and viral miRNAs and lncRNAs. The samples clustered strongly and, of the 754 cellular miRNAs studied, 24 were significantly up-regulated and 50 down-regulated. Our results confirmed data in the literature on some miRNAs (miR-223*, miR-151-3p, miR-151-5p, miR-28-5p, miR-99a), known to regulate LCL immortalization [38].

The viral miRNA analysis showed that only a part of the 44 EBV miRNAs were amplified (EBV- miR-BHRF1-1, miR-BHRF1-2 and miR-BHRF1-3 of the BHRF cluster, ebv-BART1-3p, BART1-5p, BART2-5p, BART3, BART3*, BART4 and BART15 of the BART cluster), and these results are consistent with the deletion of 12 Kb in the BamHI-A region carried from the EBV B95.8 strain [28,70].

We were also interested in the lncRNA content, transcripts >200 nt in length [29], since little is known about their role in LCL generation. We found that the lncRNAs 7SL, H19, H19 antisense and p53mRNA showed a higher expression in the autologous LCL when compared with PBMC. It is known that these lncRNAs are involved in tumorigenesis, suggesting their possible role in LCL generation and, in general, their contribution to EBV-driven tumorigenesis.

Interestingly, the 7SL expression levels were found to be significantly elevated in EBV-infected cells because the promoter sequences of its gene are similar to those of EBER genes [19]. Moreover, ncRNA 7SL is up-regulated in cancer cells [14], where it represses p53 translation [1].

H19 is considered one of the major cancer genes because of its critical role in all stages of tumorigenesis, and its high expression in almost every human cancer [48,63].

We also found an upregulation of the messenger RNA that encodes the p53 protein (p53 mRNA), which also has a regulatory role in interacting with Mdm2 protein, controlling its function and p53 gene expression [11]. The transcription of p53 in EBV-infected B cells is a host response to the infection [4,59]. LCL retain wild-type p53, but it is inhibited by MDM2, and this is required for EBV-driven

Please cite this article in press as: A. Gallo, et al., Global profiling of viral and cellular non-coding RNAs in Epstein–Barr virus-induced lymphoblastoid cell lines and released exosome cargos, Cancer Letters (2016), http://dx.doi.org/10.1016/j.canlet.2016.12.003

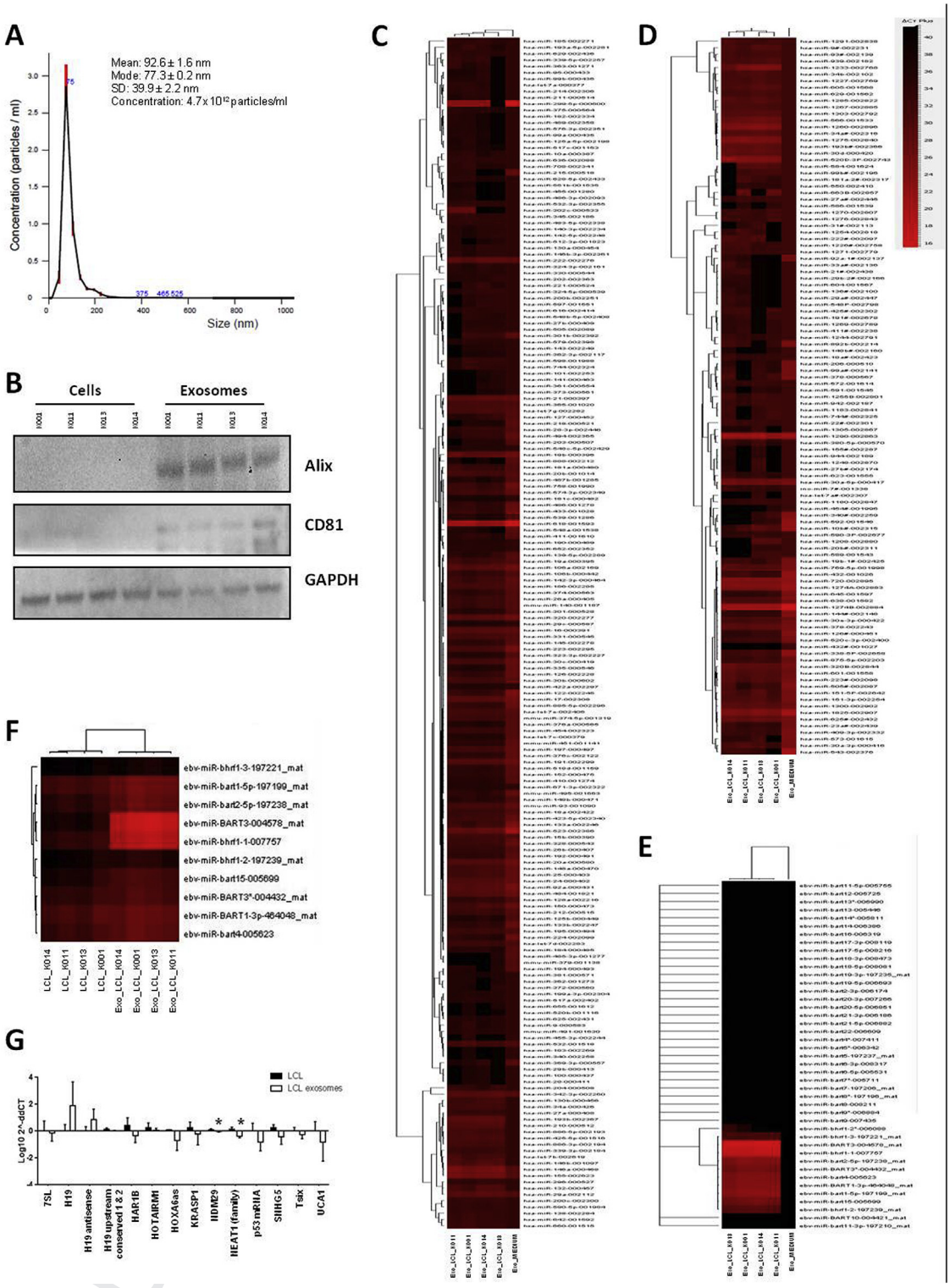

Fig. 2. A. NanoSight measurement of particle-size distribution in LCL exosome preparations. Data are mean values (n = 5) ± SD. **B**. Western blot analysis of CD81, Alix and GAPDH in whole LCL cells (n = 4) and their exosomes (n = 4). The purity of exosome fractions was determined by the presence of multivesicular body-derived Alix and CD81 proteins. **C and D**. Heat map representation of differentially regulated cellular miRNAs performed on RNA extracted from exosomes of LCL (n = 4) or those of the non-conditioned medium, using TaqMan® Low Density Array (TLDA). Heat map shows the expression of the 754 cellular miRNAs (pool A and pool B, Figures **C** and **D**, respectively), which highlighted significantly regulated expression between LCL exosomes and non-conditioned medium. The distance measured is Pearson's Distance, and the clustering method is average linkage. Branch lengths represent the degree of similarity between individual samples (Top) or miRNA (Left). Red and black colors indicate relatively high and low expression, respectively. **E and F**. Expression profile of EBV-specific microRNAs in LCL exosomes (n = 4) compared to those of the-non conditioned medium (Figure **E**) or to LCL (Figure **F**). Expression data of 44 viral miRNAs were obtained with Custom TaqMan® Array MicroRNA Cards (Life Technologies. Thermo Fisher Scientific), and the results are shown in the heat map. The distance measured is Pearson's Distance, and the clustering method is average linkage. Dendrograms of clustering analysis for samples and miRNAs are displayed on the top and left, respectively. Red and black colors indicate relatively high and low expression, respectively. **G**. LCL and their exosomes differentially express cellular lncRNAs. The graph shows quantitative RT-PCR results of RNA extracted from LCL (n = 4) and their exosomes (n = 4). Results are displayed as mean levels and SD relative to the average expression of LCL, and are normalized to GAPDH. One star (*) indicates a $p < 0.05$ on two-tailed Student's test. (For interpretation of the references to colour in this figure legend, the reader is referred to the web version of this article.)

Please cite this article in press as: A. Gallo, et al., Global profiling of viral and cellular non-coding RNAs in Epstein–Barr virus-induced lymphoblastoid cell lines and released exosome cargos, Cancer Letters (2016), http://dx.doi.org/10.1016/j.canlet.2016.12.003

transformation and survival of the infected cells [20]. It is known that many virally infected cells secrete not only viral particles, but also microvesicles that contain various viral proteins and RNAs [2,12,24,34]. Microvesicles exert their biological functions through interactions with recipient cells, and by transfer of multiple molecules as soluble and insoluble factors [71], mRNA and miRNAs [17,40,51,58,82].

The microvesicle transfer of viral and cellular factors, particularly in the case of persistent infections, such as those of the herpesviruses, would allow the virus to respond to or control the cellular microenvironment, which could be beneficial both to the virus and to the host, as this could potentially reduce viral replication to a minimum [50].

Notably, exosomes contribute to tumorigenesis process and tumor immune escape [32,83], as demonstrated in many cancer types [5,30,45,61,71]. Very recently, it has been also demonstrated that exosomes derived from tumor cells are able to induce morphological and functional changes in mesenchymal stem cells, favouring tumor growth and the malignant progression [44].

These findings suggest that exosomes released by EBV-infected cells could have an important role in tumorigenic and metastasis potential of this virus.

Due to the role that the LCL exosomal cargo transfer might play in maintaining the persistent infection [3], and in inducing tumorigenesis [84], we wanted to characterize the exosomal ncRNA cargo released from LCL. We identified the presence of RNA molecules involved in post-transcriptional regulation (miRNAs and lncRNAs) in purified exosomes from LCL transformed by the B95-8 strain of EBV. Recently, Canitano analyzed a panel of only five EBV-encoded miRNAs in an LCL [12], and the results are in line with ours.

We assessed that all the viral miRNAs expressed by LCL are also packaged in the exosomes, and we explored the possibility of a specific viral miRNA packaging process. We compared the viral miRNA expression of LCL with their released exosomes, and found that 2 miRNAs, ebv-miR-BART3 and ebv-miR-BHRF1-1, are highly differentially expressed. It has been demonstrated that EBV-miR-BART3 targets importin 7 (IPO7), induces the pro-inflammatory cytokine IL-6, and is implicated in the regulation of innate immunity [8]. Moreover, it targets caspase 3 exerting an anti-apoptotic effect [25], confirming previous results. The BHRF1 miRNA cluster appears to strongly potentiate the transforming properties of EBV, and in particular it has been found that miR-BHRF1-1 potentiates viral lytic replication by down-regulating host p53 in nasopharyngeal carcinoma [42]. The abundance of these specific EBV-miRNAs might suggest a microvescicular transfer potentially functioning not only in the infected cell, but also in neighbouring or even distant cells following a paracrine mechanism.

We also profiled the cellular miRNAs found in the exosomal fraction. We found present only 304 of the 751 miRNAs analyzed, showing a clear distinct panel of miRNAs packaged in the exosomes, in strong agreement with data in the literature.

We found, for the first time to our knowledge, the presence of lncRNA sequences within LCL exosomes (7SL, H19, H19 upstream conserved 1&2, H19 antisense, HAR1B, HOXA6as, NDM29, SNHG5 and Tsix). In addition, lncRNA profiling revealed that LCL were enriched in lncRNA H19 and H19 antisense, and released these through exosomes, suggesting a leading role in the regulation of the tumor microenvironment, as previously reported [15]. Though future functional studies will be necessary to discover the mechanisms in which these ncRNAs are involved, and to determine their role in carcinogenesis, this study further emphasizes the potential role of ncRNAs and exosomal transfer in EBV biology and in tumorigenesis, and provides a comprehensive characterization of LCL and their exosome cargos.

Acknowledgements

This work is part of the project "MIRCO CUP – G71I14000010007", granted by the Sicilian Region under the European Regional Development Fund (ERDF) – funding Programme "PO FESR 2007–2013".

We would like to thank G. Zito and R. Alessandro for providing the antibodies for the exosomal fraction characterization. We thank Warren Blumberg for assistance in editing the manuscript. Q6

Conflict of interest Q5

The authors declare no conflict of interest.

Appendix A. Supplementary data

Supplementary data related to this article can be found at http://dx.doi.org/10.1016/j.canlet.2016.12.003.

References

[1] K. Abdelmohsen, A.C. Panda, M.J. Kang, R. Guo, J. Kim, I. Grammatikakis, et al., 7SL RNA represses p53 translation by competing with HuR, Nucleic Acids Res. 42 (2014) 10099–10111.
[2] W. Ahmed, P.S. Philip, S. Tariq, G. Khan, Epstein-Barr virus-encoded small RNAs (EBERs) are present in fractions related to exosomes released by EBV-transformed cells, PloS One 9 (2014) e99163.
[3] M. Alenquer, M.J. Amorim, Exosome biogenesis, regulation, and function in viral infection, Viruses 7 (2015) 5066–5083.
[4] M.J. Allday, A. Sinclair, G. Parker, D.H. Crawford, P.J. Farrell, Epstein-Barr virus efficiently immortalizes human B cells without neutralizing the function of p53, EMBO J. 14 (1995) 1382–1391.
[5] G. Andreola, L. Rivoltini, C. Castelli, V. Huber, P. Perego, P. Deho, et al., Induction of lymphocyte apoptosis by tumor cell secretion of FasL-bearing microvesicles, J. Exp. Med. 195 (2002) 1303–1316.
[6] G.J. Babcock, L.L. Decker, M. Volk, D.A. Thorley-Lawson, EBV persistence in memory B cells in vivo, Immunity 9 (1998) 395–404.
[7] S.Y. Baik, H.S. Yun, H.J. Lee, M.H. Lee, S.E. Jung, J.W. Kim, et al., Identification of stathmin 1 expression induced by Epstein-Barr virus in human B lymphocytes, Cell Prolif. 40 (2007) 268–281.
[8] S. Barth, G. Meister, F.A. Grasser, EBV-encoded miRNAs, Biochim. Biophys. Acta 1809 (2011) 631–640.
[9] S.H. Bernacki, J.C. Beck, K. Muralidharan, F.V. Schaefer, A.E. Shrimpton, K.L. Richie, et al., Characterization of publicly available lymphoblastoid cell lines for disease-associated mutations in 11 genes, Clin. Chem. 51 (2005) 2156–2159.
[10] A. Bobrie, M. Colombo, S. Krumeich, G. Raposo, C. Thery, Diverse subpopulations of vesicles secreted by different intracellular mechanisms are present in exosome preparations obtained by differential ultracentrifugation, J. Extracell. Vesicles 1 (2012).
[11] M.M. Candeias, L. Malbert-Colas, D.J. Powell, C. Daskalogianni, M.M. Maslon, N. Naski, et al., P53 mRNA controls p53 activity by managing Mdm2 functions, Nat. Cell Biol. 10 (2008) 1098–1105.
[12] A. Canitano, G. Venturi, M. Borghi, M.G. Ammendolia, S. Fais, Exosomes released in vitro from Epstein-Barr virus (EBV)-infected cells contain EBV-encoded latent phase mRNAs, Cancer Lett. 337 (2013) 193–199.
[13] H.S. Chahar, X. Bao, A. Casola, Exosomes and their role in the life cycle and pathogenesis of RNA viruses, Viruses 7 (2015) 3204–3225.
[14] W. Chen, W. Bocker, J. Brosius, H. Tiedge, Expression of neural BC200 RNA in human tumours, J. Pathol. 183 (1997) 345–351.
[15] A. Conigliaro, V. Costa, A. Lo Dico, L. Saieva, S. Buccheri, F. Dieli, et al., CD90+ liver cancer cells modulate endothelial cell phenotype through the release of exosomes containing H19 lncRNA, Mol. Cancer 14 (2015) 155.
[16] R. Dolcetti, Cross-talk between Epstein-Barr virus and microenvironment in the pathogenesis of lymphomas, Semin. Cancer Biol. 34 (2015) 58–69.
[17] S. Fais, L. O'Driscoll, F.E. Borras, E. Buzas, G. Camussi, F. Cappello, et al., Evidence-based clinical use of nanoscale extracellular vesicles in nanomedicine, ACS Nano 10 (2016) 3886–3899.
[18] R. Feederle, S.D. Linnstaedt, H. Bannert, H. Lips, M. Bencun, B.R. Cullen, et al., A viral microRNA cluster strongly potentiates the transforming properties of a human herpesvirus, PLoS Pathog. 7 (2011) e1001294.
[19] Z.A. Felton-Edkins, A. Kondrashov, D. Karali, J.A. Fairley, C.W. Dawson, J.R. Arrand, et al., Epstein-Barr virus induces cellular transcription factors to allow active expression of EBER genes by RNA polymerase III, J. Biol. Chem. 281 (2006) 33871–33880.
[20] E. Forte, M.A. Luftig, MDM2-dependent inhibition of p53 is required for Epstein-Barr virus B-cell growth transformation and infected-cell survival, J. Virol. 83 (2009) 2491–2499.

[21] A. Gallo, I. Alevizos, Isolation of circulating microRNA in saliva, Methods Mol. Biol. 1024 (2013) 183–190.
[22] A. Gallo, M. Tandon, I. Alevizos, G.G. Illei, The majority of microRNAs detectable in serum and saliva is concentrated in exosomes, PloS One 7 (2012) e30679.
[23] E.A. Gibb, C.J. Brown, W.L. Lam, The functional role of long non-coding RNA in human carcinomas, Mol. Cancer 10 (2011) 38.
[24] C. Gourzones, A. Gelin, I. Bombik, J. Klibi, B. Verillaud, J. Guigay, et al., Extracellular release and blood diffusion of BART viral micro-RNAs produced by EBV-infected nasopharyngeal carcinoma cells, Virol. J. 7 (2010) 271.
[25] C. Harold, D. Cox, K.J. Riley, Epstein-Barr viral microRNAs target caspase 3, Virol. J. 13 (2016) 145.
[26] J.T. Herbeck, G.S. Gottlieb, K. Wong, R. Detels, J.P. Phair, C.R. Rinaldo, et al., Fidelity of SNP array genotyping using Epstein Barr virus-transformed B-lymphocyte cell lines: implications for genome-wide association studies, PloS One 4 (2009) e6915.
[27] M. Hijikata, Y.K. Shimizu, H. Kato, A. Iwamoto, J.W. Shih, H.J. Alter, et al., Equilibrium centrifugation studies of hepatitis C virus: evidence for circulating immune complexes, J. Virol. 67 (1993) 1953–1958.
[28] M.J. Hooykaas, E. Kruse, E.J. Wiertz, R.J. Lebbink, Comprehensive profiling of functional Epstein-Barr virus miRNA expression in human cell lines, BMC Genom. 17 (2016) 644.
[29] Y. Huang, N. Liu, J.P. Wang, Y.Q. Wang, X.L. Yu, Z.B. Wang, et al., Regulatory long non-coding RNA and its functions, J. Physiol. Biochem. 68 (2012) 611–618.
[30] V. Huber, S. Fais, M. Iero, L. Lugini, P. Canese, P. Squarcina, et al., Human colorectal cancer cells induce T-cell death through release of proapoptotic microvesicles: role in immune escape, Gastroenterology 128 (2005) 1796–1804.
[31] T. Hussain, R. Mulherkar, Lymphoblastoid cell lines: a continuous in vitro source of cells to study carcinogen sensitivity and DNA repair, Int. J. Mol. Cell. Med. 1 (2012) 75–87.
[32] M. Iero, R. Valenti, V. Huber, P. Filipazzi, G. Parmiani, S. Fais, et al., Tumour-released exosomes and their implications in cancer immunity, Cell Death Differ. 15 (2008) 80–88.
[33] T. Katsuda, R. Tsuchiya, N. Kosaka, Y. Yoshioka, K. Takagaki, K. Oki, et al., Human adipose tissue-derived mesenchymal stem cells secrete functional neprilysin-bound exosomes, Sci. Rep. 3 (2013) 1197.
[34] C. Keryer-Bibens, C. Pioche-Durieu, C. Villemant, S. Souquere, N. Nishi, M. Hirashima, et al., Exosomes released by EBV-infected nasopharyngeal carcinoma cells convey the viral latent membrane protein 1 and the immunomodulatory protein galectin 9, BMC Cancer 6 (2006) 283.
[35] G. Khan, M.J. Hashim, Global burden of deaths from Epstein-Barr virus attributable malignancies 1990–2010, Infect. Agents Cancer 9 (2014) 38.
[36] D. Koppers-Lalic, M. Hackenberg, I.V. Bijnsdorp, M.A. van Eijndhoven, P. Sadek, D. Sie, et al., Nontemplated nucleotide additions distinguish the small RNA composition in cells from exosomes, Cell Rep. 8 (2014) 1649–1658.
[37] J.C. Latourelle, N. Pankratz, A. Dumitriu, J.B. Wilk, S. Goldwurm, G. Pezzoli, et al., Genomewide association study for onset age in Parkinson disease, BMC Med. Genet. 10 (2009) 98.
[38] J.E. Lee, E.J. Hong, H.Y. Nam, J.W. Kim, B.G. Han, J.P. Jeon, MicroRNA signatures associated with immortalization of EBV-transformed lymphoblastoid cell lines and their clinical traits, Cell Prolif. 44 (2011) 59–66.
[39] J.E. Lee, H.Y. Nam, S.M. Shim, G.R. Bae, B.G. Han, J.P. Jeon, Expression phenotype changes of EBV-transformed lymphoblastoid cell lines during long-term subculture and its clinical significance, Cell Prolif. 43 (2010) 378–384.
[40] T. Lener, M. Gimona, L. Aigner, V. Borger, E. Buzas, G. Camussi, et al., Applying extracellular vesicles based therapeutics in clinical trials – an ISEV position paper, J. Extracell. Vesicles 4 (2015) 30087.
[41] J. Li, Z. Xuan, C. Liu, Long non-coding RNAs and complex human diseases, Int. J. Mol. Sci. 14 (2013) 18790–18808.
[42] Z. Li, X. Chen, L. Li, S. Liu, L. Yang, X. Ma, et al., EBV encoded miR-BHRF1-1 potentiates viral lytic replication by downregulating host p53 in nasopharyngeal carcinoma, Int. J. Biochem. Cell Biol. 44 (2012) 275–279.
[43] E.R. Londin, M.A. Keller, M.R. D'Andrea, K. Delgrosso, A. Ertel, S. Surrey, et al., Whole-exome sequencing of DNA from peripheral blood mononuclear cells (PBMC) and EBV-transformed lymphocytes from the same donor, BMC Genom. 12 (2011) 464.
[44] L. Lugini, M. Valtieri, C. Federici, S. Cecchetti, S. Meschini, M. Condello, et al., Exosomes from human colorectal cancer induce a tumor-like behavior in colonic mesenchymal stromal cells, Oncotarget (2016).
[45] M. Lundholm, M. Schroder, O. Nagaeva, V. Baranov, A. Widmark, L. Mincheva-Nilsson, et al., Prostate tumor-derived exosomes down-regulate NKG2D expression on natural killer cells and CD8+ T cells: mechanism of immune evasion, PloS One 9 (2014) e108925.
[46] F. Marques-Garcia, M. Isidoro-Garcia, Protocols for exosome isolation and RNA profiling, Methods Mol. Biol. 1434 (2016) 153–167.
[47] O.M. Martinez, F.R. de Gruijl, Molecular and immunologic mechanisms of cancer pathogenesis in solid organ transplant recipients, Am. J. Transplant. Off. J. Am. Soc. Transplant. Am. Soc. Transplant. Surg. 8 (2008) 2205–2211.
[48] I.J. Matouk, N. DeGroot, S. Mezan, S. Ayesh, R. Abu-lail, A. Hochberg, et al., The H19 non-coding RNA is essential for human tumor growth, PloS One 2 (2007) e845.
[49] N.S. McCarthy, S.M. Allan, D. Chandler, A. Jablensky, B. Morar, Integrity of genome-wide genotype data from low passage lymphoblastoid cell lines, Genom. Data 9 (2016) 18–21.
[50] D.G. Meckes Jr., N. Raab-Traub, Microvesicles and viral infection, J. Virol. 85 (2011) 12844–12854.
[51] D.G. Meckes Jr., K.H. Shair, A.R. Marquitz, C.P. Kung, R.H. Edwards, N. Raab-Traub, Human tumor virus utilizes exosomes for intercellular communication, Proc. Natl. Acad. Sci. U. S. A. 107 (2010) 20370–20375.
[52] S. Metzenberg, Levels of Epstein-Barr virus DNA in lymphoblastoid cell lines are correlated with frequencies of spontaneous lytic growth but not with levels of expression of EBNA-1, EBNA-2, or latent membrane protein, J. Virol. 64 (1990) 437–444.
[53] G. Miller, M. Lipman, Release of infectious Epstein-Barr virus by transformed marmoset leukocytes, Proc. Natl. Acad. Sci. U. S. A. 70 (1973) 190–194.
[54] G. Miller, T. Shope, H. Lisco, D. Stitt, M. Lipman, Epstein-Barr virus: transformation, cytopathic changes, and viral antigens in squirrel monkey and marmoset leukocytes, Proc. Natl. Acad. Sci. U. S. A. 69 (1972) 383–387.
[55] A. Mohyuddin, Q. Ayub, S. Siddiqi, D.R. Carvalho-Silva, K. Mazhar, S. Rehman, et al., Genetic instability in EBV-transformed lymphoblastoid cell lines, Biochim. Biophys. Acta 1670 (2004) 81–83.
[56] G.W. Montgomery, M.J. Campbell, P. Dickson, S. Herbert, K. Siemering, K.R. Ewen-White, et al., Estimation of the rate of SNP genotyping errors from DNA extracted from different tissues, Twin Res. Hum. Genet. Off. J. Int. Soc. Twin Stud. 8 (2005) 346–352.
[57] H. Neitzel, A routine method for the establishment of permanent growing lymphoblastoid cell lines, Hum. Genet. 73 (1986) 320–326.
[58] D.M. Pegtel, K. Cosmopoulos, D.A. Thorley-Lawson, M.A. van Eijndhoven, E.S. Hopmans, J.L. Lindenberg, et al., Functional delivery of viral miRNAs via exosomes, Proc. Natl. Acad. Sci. U. S. A. 107 (2010) 6328–6333.
[59] K. Pokrovskaja, I. Okan, E. Kashuba, M. Lowbeer, G. Klein, L. Szekely, Epstein-Barr virus infection and mitogen stimulation of normal B cells induces wild-type p53 without subsequent growth arrest or apoptosis, J. General Virol. 80 (Pt 4) (1999) 987–995.
[60] V.M. Pratt, B. Zehnbauer, J.A. Wilson, R. Baak, N. Babic, M. Bettinotti, et al., Characterization of 107 genomic DNA reference materials for CYP2D6, CYP2C19, CYP2C9, VKORC1, and UGT1A1: a GeT-RM and Association for Molecular Pathology collaborative project, J. Mol. Diagn. JMD 12 (2010) 835–846.
[61] G. Rabinowits, C. Gercel-Taylor, J.M. Day, D.D. Taylor, G.H. Kloecker, Exosomal microRNA: a diagnostic marker for lung cancer, Clin. Lung Cancer 10 (2009) 42–46.
[62] G. Raposo, H.W. Nijman, W. Stoorvogel, R. Liejendekker, C.V. Harding, C.J. Melief, et al., B lymphocytes secrete antigen-presenting vesicles, J. Exp. Med. 183 (1996) 1161–1172.
[63] E. Raveh, I.J. Matouk, M. Gilon, A. Hochberg, The H19 long non-coding RNA in cancer initiation, progression and metastasis – a proposed unifying theory, Mol. Cancer 14 (2015) 184.
[64] E. Seto, A. Moosmann, S. Gromminger, N. Walz, A. Grundhoff, W. Hammerschmidt, Micro RNAs of Epstein-Barr virus promote cell cycle progression and prevent apoptosis of primary human B cells, PLoS Pathog. 6 (2010) e1001063.
[65] L. Sie, S. Loong, E.K. Tan, Utility of lymphoblastoid cell lines, J. Neurosci. Res. 87 (2009) 1953–1959.
[66] J. Simon-Sanchez, S. Scholz, H.C. Fung, M. Matarin, D. Hernandez, J.R. Gibbs, et al., Genome-wide SNP assay reveals structural genomic variation, extended homozygosity and cell-line induced alterations in normal individuals, Hum. Mol. Genet. 16 (2007) 1–14.
[67] J. Simon-Sanchez, C. Schulte, J.M. Bras, M. Sharma, J.R. Gibbs, D. Berg, et al., Genome-wide association study reveals genetic risk underlying Parkinson's disease, Nat. Genet. 41 (2009) 1308–1312.
[68] D.L. Sitki-Green, R.H. Edwards, M.M. Covington, N. Raab-Traub, Biology of Epstein-Barr virus during infectious mononucleosis, J. Infect. Dis. 189 (2004) 483–492.
[69] R.L. Skalsky, D.L. Corcoran, E. Gottwein, C.L. Frank, D. Kang, M. Hafner, et al., The viral and cellular microRNA targetome in lymphoblastoid cell lines, PLoS Pathog. 8 (2012) e1002484.
[70] J. Skare, C. Edson, J. Farley, J.L. Strominger, The B95-8 isolate of Epstein-Barr virus arose from an isolate with a standard genome, J. Virol. 44 (1982) 1088–1091.
[71] J. Skog, T. Wurdinger, S. van Rijn, D.H. Meijer, L. Gainche, M. Sena-Esteves, et al., Glioblastoma microvesicles transport RNA and proteins that promote tumour growth and provide diagnostic biomarkers, Nat. Cell Biol. 10 (2008) 1470–1476.
[72] A.L. Stark, W. Zhang, T. Zhou, P.H. O'Donnell, C.M. Beiswanger, R.S. Huang, et al., Population differences in the rate of proliferation of international HapMap cell lines, Am. J. Hum. Genet. 87 (2010) 829–833.
[73] M. Sugimoto, H. Tahara, T. Ide, Y. Furuichi, Steps involved in immortalization and tumorigenesis in human B-lymphoblastoid cell lines transformed by Epstein-Barr virus, Cancer Res. 64 (2004) 3361–3364.
[74] X.L. Tan, A.M. Moyer, B.L. Fridley, D.J. Schaid, N. Niu, A.J. Batzler, et al., Genetic variation predicting cisplatin cytotoxicity associated with overall survival in lung cancer patients receiving platinum-based chemotherapy, Clin. Cancer Res. Off. J. Am. Assoc. Cancer Res. 17 (2011) 5801–5811.
[75] D.A. Thorley-Lawson, Epstein-Barr virus: exploiting the immune system, Nat. Rev. Immunol. 1 (2001) 75–82.
[76] T. Toda, M. Sugimoto, Proteome analysis of Epstein-Barr virus-transformed B-lymphoblasts and the proteome database, J. Chromatogr. B Anal. Technol. Biomed. Life Sci. 787 (2003) 197–206.

Please cite this article in press as: A. Gallo, et al., Global profiling of viral and cellular non-coding RNAs in Epstein–Barr virus-induced lymphoblastoid cell lines and released exosome cargos, Cancer Letters (2016), http://dx.doi.org/10.1016/j.canlet.2016.12.003

[77] H. Vallhov, C. Gutzeit, S.M. Johansson, N. Nagy, M. Paul, Q. Li, et al., Exosomes containing glycoprotein 350 released by EBV-transformed B cells selectively target B cells through CD21 and block EBV infection in vitro, J. Immunol. 186 (2011) 73–82.

[78] G. Vazirabadi, T.R. Geiger, W.F. Coffin 3rd, J.M. Martin, Epstein-Barr virus latent membrane protein-1 (LMP-1) and lytic LMP-1 localization in plasma membrane-derived extracellular vesicles and intracellular virions, J. General Virol. 84 (2003) 1997–2008.

[79] Z. Wei, A.O. Batagov, D.R. Carter, A.M. Krichevsky, Fetal bovine serum RNA interferes with the cell culture derived extracellular RNA, Sci. Rep. 6 (2016) 31175.

[80] M. Welsh, L. Mangravite, M.W. Medina, K. Tantisira, W. Zhang, R.S. Huang, et al., Pharmacogenomic discovery using cell-based models, Pharmacol. Rev. 61 (2009) 413–429.

[81] H.E. Wheeler, M.E. Dolan, Lymphoblastoid cell lines in pharmacogenomic discovery and clinical translation, Pharmacogenomics 13 (2012) 55–70.

[82] M. Yanez-Mo, P.R. Siljander, Z. Andreu, A.B. Zavec, F.E. Borras, E.I. Buzas, et al., Biological properties of extracellular vesicles and their physiological functions, J. Extracell. Vesicles 4 (2015) 27066.

[83] H.G. Zhang, W.E. Grizzle, Exosomes: a novel pathway of local and distant intercellular communication that facilitates the growth and metastasis of neoplastic lesions, Am. J. Pathol. 184 (2014) 28–41.

[84] X. Zhang, X. Yuan, H. Shi, L. Wu, H. Qian, W. Xu, Exosomes in cancer: small particle, big player, J. Hematol. Oncol. 8 (2015) 83.

[85] A. Zijno, P. Porcedda, F. Saini, A. Allione, B. Garofalo, F. Marcon, et al., Unsuitability of lymphoblastoid cell lines as surrogate of cryopreserved isolated lymphocytes for the analysis of DNA double-strand break repair activity, Mutat. Res. 684 (2010) 98–105.

Please cite this article in press as: A. Gallo, et al., Global profiling of viral and cellular non-coding RNAs in Epstein–Barr virus-induced lymphoblastoid cell lines and released exosome cargos, Cancer Letters (2016), http://dx.doi.org/10.1016/j.canlet.2016.12.003